DOI: 10.1061/(ASCE)MT.1943-5533.0003052

ASCE

Evaluation of Elastic Anisotropy of Concrete Using Ultrasound Wave Propagation

Cinthya Bertoldo, Ph.D.[1]; Recieli Knoner Santos Gorski[2]; and Raquel Gonçalves, Ph.D.[3]

Abstract: The aim of this study was to test the isotropic behavior hypothesis for concrete by means of wave propagation tests. The elastic properties of the concrete were determined using ultrasound tests with 1.0 MHz longitudinal and transversal transducers in polyhedral specimens with 26 faces. The concrete was analyzed using the theoretical aspects of three types of elastic behavior, namely isotropy, transverse isotropy, and orthotropy, in concretes with different compressive strengths and coarse aggregate size distributions. The results show that there were no statistically significant differences in the elastic parameters on the three symmetry axes. The constitutive relation between the shear modulus and longitudinal modulus, which involves Poisson's ratio, was as expected for isotropic materials, and the elastic properties of the concrete differed equally as a function of the compressive strength. Considering the results, the isotropic behavior of the concrete was validated regardless of the elastic behavior adopted in the analyses. **DOI: 10.1061/(ASCE)MT.1943-5533.0003052.** © *2020 American Society of Civil Engineers.*

Introduction

Concrete is a widely disseminated material, and one of the most highly consumed materials in the world due to several factors, including its flexibility in structural design and its structural performance in different environments (Isaia 2017). As a result, numerous studies have focused on this material to understand its microstructural complexity and to test new compositions. However, concrete is generally assumed, without much questioning, to display isotropic behavior, even though its heterogeneity and specific aspects of its molding have been recognized.

Elastic anisotropy defines a material based on its response to stresses in different directions. An anisotropic material is one in which the elastic properties vary in different directions, and anisotropy occurs in materials with a defined internal structure, such as wood (which is considered orthotropic). Thus, for wood, the values of the elasticity moduli in the x-, y-, and z-directions are different. A simpler material is one that exhibits isotropic behavior, with equal responses by the properties in all directions. When a material responds differently in two of the three directions, it is said to have transverse isotropy.

For structural purposes, concrete is assumed to be isotropic, and it is considered to have transverse or orthotropic isotropy only after suffering damage (Rashid 1968; Papa and Taliercio 1996; Cicekli et al. 2007). However, the assumption of isotropic behavior may not be appropriate because, for example, of compaction. The direction of the compaction has a nonnegligible effect on the expected isotropic behavior of concrete because the action of gravity favors compaction along one of the axes (Torrenti et al. 2013). In addition, by inserting concrete into a mold in the direction of compaction, the air bubbles that form may be prevented from rising to the surface and may become blocked and cause oriented defects under the aggregate layer, which may initiate microcracks in the same direction and thus modify the expected isotropic conditions (Torrenti et al. 2013). This phenomenon gives rise to the so-called initial anisotropy of concrete, which leads to differences in the properties in the direction of compaction and in the directions perpendicular to compaction, both for the strength (compressive and tensile) (Hughes and Ash 1970) and the elastic properties (Torrenti et al. 2013). Torrenti et al. (2013) noted that these differences tend to increase with increases in the water-cement factor.

The difficulty in obtaining the elastic parameters of a material (the longitudinal moduli of elasticity in different directions, the transverse moduli of elasticity on different planes and Poisson's ratios) depends on the complexity of the material in terms of the elastic anisotropy. Twelve constants are required to describe the elastic behavior of an orthotropic material, namely three longitudinal moduli of elasticity (E_1, E_2, and E_3), three transverse moduli of elasticity (G_{12}, G_{13}, and G_{23}) and six Poisson's ratios (μ_{12}, μ_{21}, μ_{23}, μ_{32}, μ_{13}, and μ_{31}). In materials with transverse isotropy and two planes with equal responses to the actions (e.g., Planes 1 and 2), the rigidity matrix is simplified; it is composed of seven elements ($E_1 = E_2$, E_3, G_{12}, $G_{13} = G_{23}$, $\mu_{12} = \mu_{21}$, $\mu_{13} = \mu_{23}$, $\mu_{31} = \mu_{32}$), five of which are independent. Finally, in the case of isotropic materials, the matrix has only three elements ($E_1 = E_2 = E_3$; $G_{12} = G_{13} = G_{23}$; and $\mu_{12} = \mu_{21} = \mu_{23} = \mu_{32} = \mu_{13} = \mu_{31}$), two of which are independent.

Determining these constants using static methods, such as compression testing, is feasible but cumbersome, and it is complex in terms of the required equipment (the testing machine and data acquisition system) and costly because it is necessary to use many strain gauges, which are discarded after the test has been performed.

[1]Assistant Professor, Laboratory of Nondestructive Testing, School of Agricultural Engineering—FEAGRI, Univ. of Campinas, Ave. Cândido Rondon, 501, Barão Geraldo 13083-875, Campinas, Brazil (corresponding author). ORCID: https://orcid.org/0000-0001-9039-4805. Email: cinthyab@unicamp.br

[2]Master, Laboratory of Nondestructive Testing, School of Agricultural Engineering—FEAGRI, Univ. of Campinas, Ave. Cândido Rondon, 501, Barão Geraldo 13083-875, Campinas, Brazil. Email: reciksantos@gmail.com

[3]Professor, Laboratory of Nondestructive Testing, School of Agricultural Engineering—FEAGRI, Univ. of Campinas, Ave. Cândido Rondon, 501, Barão Geraldo 13083-875, Campinas, Brazil. ORCID: https://orcid.org/0000-0003-0406-8988. Email: raquelg@unicamp.br

Note. This manuscript was submitted on March 22, 2019; approved on July 30, 2019; published online on February 4, 2020. Discussion period open until July 4, 2020; separate discussions must be submitted for individual papers. This paper is part of the ***Journal of Materials in Civil Engineering***, © ASCE, ISSN 0899-1561.

In describing the application of ultrasound tests to concrete, Bauer (2008) shows that when a specimen is tested transversely to the concreting direction, the propagation velocity is slightly higher on average than it is in the concreting direction, which indicates nonisotropic acoustic behavior. Ultrasound data provide important information about the mechanical and elastic properties of a material (Maynard 1992; Heyliger et al. 1993; Isaak and Ohno 2003; Maynard and Liu 2012; Seiner et al. 2012; Bernard et al. 2014; Agrawal et al. 2016; Martinović et al. 2016; Liu and Shapiro 2017). Wave propagation tests are usually used to determine the elasticity of a material (Migliori et al. 1993; Ulrich et al. 2002; Migliori and Maynard 2005), its microstructure (grain size, texture, and density), and its discontinuities (porosity and damage) (Figueiredo 2005; Pereira and Medeiros 2012; Martinović et al. 2016). François et al. (1998) performed ultrasound studies on oak wood and concluded that the method was able to provide all of the elastic constants of the material using a single specimen; in addition, the method was easy to perform and reliable for the characterization of homogeneous materials. Other studies (Gonçalves et al. 2014; Vazquez et al. 2015) have successfully used the same specimen shape (polyhedral) for the complete characterization of wood by ultrasound.

Table 1. Physical, mechanical, and chemical composition (mass proportionality) of the study cement (CPII-E-32)

Parameter	Value
Fineness/residue in the sieve, 75 μm	≤12.0
Initial setting time (min)	≥60
Soundness (hot expansion) (mm)	≤5
Compressive strength (MPa)	
1 day	—
3 days	≥10.0
7 days	≥20.0
28 days	≥32.0
Clinker + calcium sulfate	51–94
Granulated blastfurnace slag (S)	6-34
Pozzolanic material	0
Fly ash	0–15
Insoluble residue	≤5.0
Sulfate content (as SO_3)	≤4.5

Table 2. Properties of the small and coarse aggregates

Aggregate	Maximum size of aggregate, MSA (mm)	Fineness modulus	Classification	Specific gravity ($kg \cdot m^{-3}$)
Sand	4.75	2.8	Upper usable zone	2,632
Gravel	9.5	6.55	Gravel 0 (G0)	2,650
Gravel	12.5	7.23	Gravel 1 (G1)	2,650

The studies discussed previously show that the behavior of concrete has been assumed to be isotropic, but no studies have empirically demonstrated this hypothesis. It is also clear that the ultrasound method has been adequate for obtaining the elastic parameters of complex materials in terms of anisotropy. The objective of this study was to test the hypothesis of the isotropic behavior of concrete using the propagation of ultrasound waves by simulating three theoretical conditions of elastic behavior, namely isotropy, transverse isotropy, and orthotropy.

Experimental and Analytical Program

Materials and Methods

CPII-E-32 cement [in accordance with ABNT NBR 16697 (ABNT 2018a) (Table 1), and derived from medium-sized sand extracted from an excavation] and basalt rock, which was used as a coarse aggregate (gravel) with two granulometries, were used to produce the concrete. The aggregates were characterized according to the Brazilian standards ABNT NBR 7211 (ABNT 2009b) and ABNT NBR NM 52 (ABNT 2009a) (Table 2).

The Brazilian Association of Portland Cement (ABCP) method was used to define the mixtures. This method is an adaptation of the American method proposed by the American Concrete Institute (ACI) for Brazilian aggregates that fall within the limits proposed by the standard [ABNT NBR 7211 (ABNT 2009b)]. The bases for determining the mixtures were 15, 25, and 35 MPa of the estimated compressive strengths ($f_{c,est}$) at 28 days, and they were calculated for concrete consistencies (slump tests) of 0.06–0.08 m (Table 3). Two mixtures for each estimated compressive strength were made, each of which had a different gravel size distribution (G0 or G1; Table 3).

To ensure the homogeneity of the mixture, all of the concrete used in this study was made in a cement mixer with an inclined axle that had a capacity of 240 L, and a vibration table was used for compaction until the concrete had a relatively smooth appearance. After 24 h of molding, the specimens were removed from the molds, identified and stored in a tank containing water according to ABNT NBR 5738 (ABNT 2015). The specimens remained in the tank until they were 28 days old. All the specimens were tested under dried conditions, approximately 10 days after being removed from the water tank, which was the necessary to prepare the polyhedron specimens.

For each estimated compressive strength (15, 25, and 35 MPa) and type of coarse aggregate (Gravel 0 and Gravel 1), nine cylindrical specimens measuring 0.10 m in diameter and 0.20 m long [ABNT NBR 5738 (ABNT 2015)] were prepared, for a total of 54 specimens. After 28 days of curing, three cylindrical specimens of each mixture (Table 3) were randomly separated. From the central part of each specimen, a 26-face polyhedron with approximately 60 mm between the faces was made [Figs. 1(a and b)]. The dimensions adopted for the specimen were defined to allow

Table 3. Estimated compressive strength ($f_{c,est}$) and the compressive strength (f_c) and mixtures used in the study

Mixture	Estimated compressive strength, $f_{c,est}$ (MPa)	Compressive strength, f_c (MPa)	Cement CPII-E-32 ($kg \cdot m^{-3}$)	Small aggregate ($kg \cdot m^{-3}$)	Coarse aggregate ($kg \cdot m^{-3}$)	Water ($kg \cdot m^{-3}$)	W/C
I	15	18	367	899	851 (Gravel 0)	220	0.60
II		21	338	767	1,055 (Gravel 1)	203	0.60
III	25	28	463	820	852 (Gravel 0)	218	0.47
IV		30	423	685	1,074 (Gravel 1)	199	0.47
V	35	35	549	851	741 (Gravel 0)	220	0.40
VI		34	501	616	1,072 (Gravel 1)	200	0.40

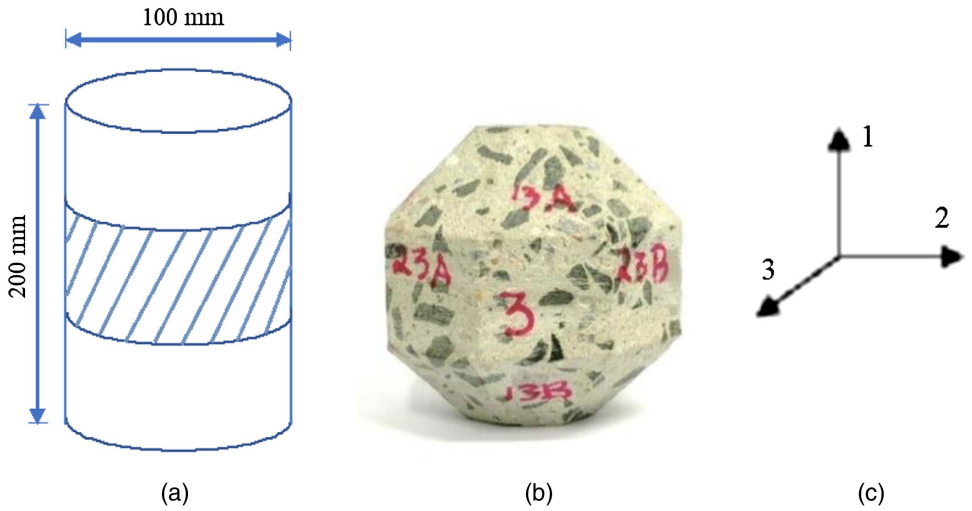

Fig. 1. Region used to make the polyhedral test specimen in the (a) cylinder; (b) concrete polyhedron with 26 faces; and (c) directions identified in the specimens.

the transducer (1.0 MHz frequency) to be circumscribed to the faces of the polyhedron. The other six cylindrical specimens were used for the static compression test and to determine the compressive resistance, f_c (Table 3) according to ABNT NBR 5739 (ABNT 2018b).

To make the polyhedron, Direction 1 was identified as the direction of the largest length (direction of compaction) of the cylindrical specimen, and the other two directions (2 and 3) were randomly marked to form three perpendicular planes [Fig. 1(c)].

The shape of the polyhedral specimen was adopted as a function of its use in the characterization of orthotropic materials, such as wood (François 1995; Trinca 2011; Gonçalves et al. 2011; Bertoldo et al. 2013; Gonçalves et al. 2014), because it allows all of the terms of the stiffness matrix to be obtained with a single specimen.

Ultrasound Testing

Ultrasound tests were performed with Epoch equipment (Epoch 1000, Olympus, Waltham, Massachusetts) and compression (longitudinal) and shear (transverse) transducers with a frequency of 1.0 MHz (Fig. 2). The coupling between the transducer and the concrete is important for the precision of the results [ABNT NBR 8802 (ABNT 2019)], and the use of viscous material is suggested to eliminate the air between the transducers and the surface of the specimen. Thus, based on Gonçalves et al. (2011), starch glucose was used as a coupling agent for the ultrasound tests, because it presents clear, representative waves and reliable peaks for shear wave recognition.

Based on ABNT NBR 8802 (ABNT 2019), Eq. (1) was used to calculate the longitudinal velocities (V_{11}, V_{22}, and V_{33}), in which the path length corresponds to the distance between the faces of the transducers, and the propagation times of the wave in Directions 1, 2, and 3, respectively, are obtained using the longitudinal transducer

$$V = \frac{L}{t} \times 10^6 \tag{1}$$

where V = wave propagation velocity in a particular direction ($m \cdot s^{-1}$); L = wave path length (m); and t = wave propagation time in a given direction (μs).

Considering the same directions but with the use of the shear transducer, the transverse velocities (V_{12}, V_{13}, V_{21}, V_{31}, V_{32}, and V_{23}) were calculated from the wave travel time (t_{12}, t_{13}, t_{21}, t_{31}, t_{32}, and t_{23}) in a given direction and its polarization was in the other two perpendicular directions. To determine the velocities corresponding to the propagation of the wave outside the symmetry axes, the wave propagation time was obtained using shear transducers on the faces oriented 45° to each plane.

Fig. 2. Ultrasound test on a polyhedral sample.

First, the stiffness matrix [C] was determined by assuming that the concrete is an orthotropic material; for this purpose, the nine independent stiffness coefficients were determined. The primary diagonal coefficients (C_{11}, C_{22}, C_{33}, C_{44}, C_{55}, and C_{66}) were obtained using the Christoffel equation [Eq. (2)]. To calculate the coefficients C_{44}, C_{55}, and C_{66}, the velocities were obtained from the shear transducer based on the times of wave propagation in the directions of the axes, the propagation of the wave in one direction, and its polarization along the two perpendicular axes. The numbering was related to the axes (propagation/polarization) as follows: 44 = Planes 2 and 3; 55 = Planes 1 and 3; and 66 = Planes 1 and 2

J. Mater. Civ. Eng., 2020, 32(4): 04020056

$$[C] = \begin{bmatrix} C_{11} & C_{12} & C_{13} & 0 & 0 & 0 \\ C_{12} & C_{22} & C_{23} & 0 & 0 & 0 \\ C_{13} & C_{23} & C_{33} & 0 & 0 & 0 \\ 0 & 0 & 0 & C_{44} & 0 & 0 \\ 0 & 0 & 0 & 0 & C_{55} & 0 \\ 0 & 0 & 0 & 0 & 0 & C_{66} \end{bmatrix}$$

$$C_{ii} = \rho \cdot V_{ii}^2 \tag{2}$$

where $i = 1, 2, 3, 4, 5$ and 6; ρ = density of the material ($\text{kg} \cdot \text{m}^{-3}$); V = wave propagation velocity in the direction being considered ($\text{m} \cdot \text{s}^{-1}$).

Eqs. (3)–(5), which were deduced from the Christoffel tensor, were used to determine the three terms that were not on the diagonal (C_{12}, C_{13}, and C_{23})

$$(C_{12} + C_{66})n_1 n_2 = [(C_{11}n_1^2 + C_{66}n_2^2 - \rho V_\alpha^2)(C_{66}n_1^2 + C_{22}n_2^2 - V_\alpha^2)]^{1/2} \tag{3}$$

$$(C_{23} + C_{44})n_2 n_3 = [(C_{22}n_2^2 + C_{44}n_3^2 - \rho V_\alpha^2)(C_{44}n_2^2 + C_{33}n_3^2 - \rho V_\alpha^2)]^{1/2} \tag{4}$$

$$(C_{13} + C_{55})n_1 n_3 = [(C_{11}n_1^2 + C_{55}n_3^2 - \rho V_\alpha^2)(C_{55}n_1^2 + C_{33}n_3^2 - \rho V_\alpha^2)]^{1/2} \tag{5}$$

where α = angle (45°); $n_1 = \cos\alpha$; $n_2 = \sin\alpha$; and $n_3 = 0$ [α is taken with respect to Axis 1] (Plane 12); $n_1 = \cos\alpha$; $n_3 = \sin\alpha$; and $n_2 = 0$ [α is taken with respect to Axis 1] (Plane 13); $n_2 = \cos\alpha$; $n_3 = \sin\alpha$; and $n_1 = 0$ [α is taken with respect to Axis 2] (Plane 23).

By inverting the $[C]^{-1}$ matrix, it was possible to obtain the flexibility matrix [S], which is associated with the elastic parameters of the material [the longitudinal modulus of elasticity (E), transverse modulus of elasticity (G), and Poisson's ratio (υ)]

$$[S] = \begin{bmatrix} \frac{1}{E_1} & -\frac{\upsilon_{21}}{E_2} & -\frac{\upsilon_{31}}{E_3} & 0 & 0 & 0 \\ -\frac{\upsilon_{12}}{E_1} & \frac{1}{E_2} & -\frac{\upsilon_{32}}{E_3} & 0 & 0 & 0 \\ -\frac{\upsilon_{13}}{E_1} & -\frac{\upsilon_{23}}{E_2} & \frac{1}{E_3} & 0 & 0 & 0 \\ 0 & 0 & 0 & \frac{1}{G_{23}} & 0 & 0 \\ 0 & 0 & 0 & 0 & \frac{1}{G_{13}} & 0 \\ 0 & 0 & 0 & 0 & 0 & \frac{1}{G_{12}} \end{bmatrix}$$

Assuming the material has transverse isotropy, Axis 1 (direction of compaction) was assumed to be different from Axes 2 and 3, which were considered to have similar properties. The same velocity data used to determine the elastic properties assuming that the concrete is orthotropic were used to determine the seven elastic properties of concrete assuming that it has transverse isotropy. However, the mean velocities were adopted for the calculations of the stiffness coefficients in the directions considered to be isotropic ($C_{22} = C_{33}$, $C_{55} = C_{66}$, and $C_{12} = C_{13}$).

When the concrete was evaluated by assuming it was isotropic, the elastic properties along Axes 1, 2, and 3 were considered equal. Thus, for the calculation of the stiffness coefficients ($C_{11} = C_{22} = C_{33}$, $C_{44} = C_{55} = C_{66}$, and $C_{23} = C_{12} = C_{13}$), the mean velocities obtained along the three symmetry axes of the polyhedron [Figs. 1(b and c)] with both the longitudinal transducer and the shear transducer were used. The velocities obtained on the inclined planes were not used in this analysis.

Analysis of Results

The results were analyzed using three treatments for the elastic parameters obtained by ultrasound and one additional analysis using compression tests (Fig. 3). In all the treatments, the statistical analysis was applied to compare the mean moduli of elasticity among the axis and shear moduli and Poisson's ratios among the planes. The statistical tests used were the t-test and the multiple range test when

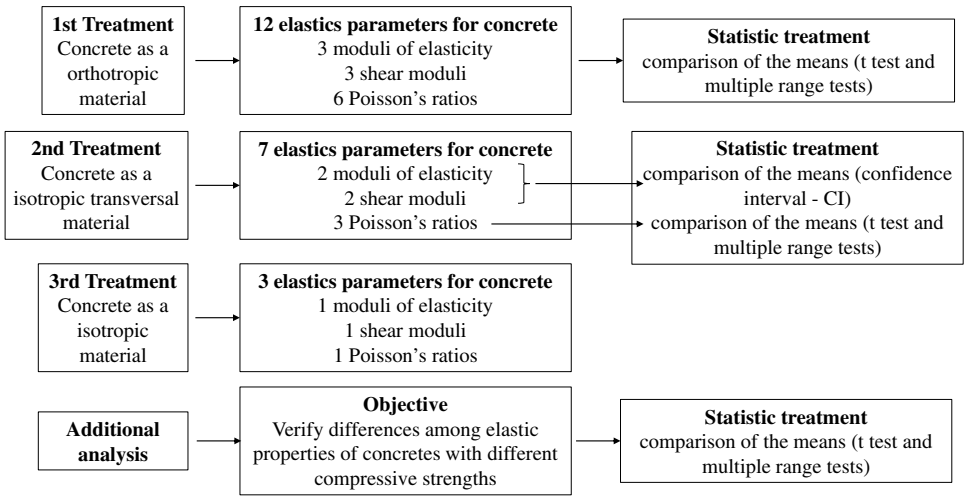

Fig. 3. Summary outline of results analysis.

the comparison involved three parameters and the confidence interval when the comparison involved two parameters.

Results and Discussion

The characterization of the concrete when viewing it as an orthotropic material (i.e., assuming it has distinct properties along the three symmetry axes) resulted in mean elasticity moduli between 27,300 and 44,400 MPa (Table 4), and the moduli varied as a function of the compressive strength of the concrete and the size distribution used in the mixture. The same results occurred with the shear moduli, which varied from 12,700 to 17,200 MPa (Table 4). The Poisson's ratio ranged from 0.08 to 0.32, and the values were below 0.14 only for concrete with compressive strengths of

Table 4. Mean results of the elastic parameters and coefficients of variation obtained for concretes with different strengths and types of gravel (G0 and G1) for the characterization considering concrete with different anisotropy conditions (orthotropy, transverse isotropy, and isotropy)

Anisotropy condition	Elastic parameters	18 MPa (G0)	21 MPa (G1)	28 MPa (G0)	30 MPa (G1)	35 MPa (G0)	34 MPa (G1)
Orthotropy	E_1 (MPa)	28,258 (Aa)	31,239 (Ba)	39,270 (Cb)	41,416 (Db)	38,859 (Eb)	38,841 (Fb)
		(3)	(9)	(8)	(2)	(1)	(6)
	E_2 (MPa)	27,745 (Aa)	34,046 (Bb)	37,646 (Cc)	40,983 (Dcd)	39,275 (Ede)	43,209 (Fe)
		(2)	(12)	(2)	(6)	(1)	(4)
	E_3 (MPa)	27,086 (Aa)	33,412 (Bb)	37,250 (Cc)	41,840 (Dcd)	38,881 (Ede)	44,397 (Fe)
		(7)	(15)	(5)	(5)	(2)	(7)
	Mean (MPa)	**27,696**	**32,899**	**38,056**	**41,413**	**39,005**	**42,149**
		(3)	**(1)**	**(4)**	**(2)**	**(1)**	**(1)**
	G_{23} (MPa)	12,788 (Ga)	14,928 (Hb)	15,074 (Ib)	15,379 (Jb)	15,695 (Kb)	17,140 (Lc)
		(1)	(8)	(1)	(5)	(0)	(4)
	G_{13} (MPa)	12,681 (Ga)	14,992 (Hb)	15,777 (Ibc)	16,225 (Jbc)	15,556 (Kbc)	16,968 (Lc)
		(1)	(9)	(9)	(8)	(1)	(5)
	G_{12} (MPa)	12,633 (Ga)	14,496 (Hb)	15,890 (Ibc)	17,216 (Jbc)	15,589 (Kc)	17,028 (Lc)
		(2)	(4)	(9)	(6)	(1)	(5)
	Mean (MPa)	**12,701**	**14,805**	**15,581**	**16,273**	**15,613**	**17,045**
		(1)	**(3)**	**(5)**	**(2)**	**(1)**	**(1)**
	ν_{21}	0.13 (MNa)	0.08 (Oa)	0.30 (PQb)	0.25 (Rb)	0.26 (Tb)	0.28 (Ub)
		(9)	(61)	(14)	(4)	(6)	(8)
	ν_{31}	0.12 (MNa)	0.14 (Oa)	0.28 (PQb)	0.26 (Rb)	0.24 (Tb)	0.28 (Ub)
		(3)	(27)	(3)	(13)	(6)	(15)
	ν_{12}	0.13 (Ma)	0.08 (Oa)	0.32 (Qb)	0.26 (Rb)	0.26 (Tb)	0.27 (Ub)
		(8)	(70)	(24)	(3)	(6)	(19)
	ν_{32}	0.11 (MNa)	0.11 (Oa)	0.24 (Pb)	0.32 (Sb)	0.24 (Tbc)	0.26 (Uc)
		(13)	(62)	(14)	(9)	(12)	(10)
	ν_{13}	0.12 (MNa)	0.13 (Oa)	0.29 (PQb)	0.26 (Rbc)	0.24 (Tbc)	0.26 (Uc)
		(1)	(25)	(16)	(7)	(4)	(5)
	ν_{23}	0.11 (Ma)	0.11 (Oa)	0.24 (PQb)	0.32 (Sbc)	0.25 (Tbc)	0.25 (Uc)
		(13)	(53)	(12)	(9)	(14)	(8)
	Mean	**0.12**	**0.11**	**0.28**	**0.28**	**0.25**	**0.27**
		(13)	**(20)**	**(8)**	**(4)**	**(4)**	**(5)**
Transverse isotropy	E_1' (MPa)	28,277	31,364	39,284	41,423	38,865	41,526
		(a)	(a)	(b)	(b)	(b)	(b)
	$E_2 = E_3$ (MPa)	27,420	33,782	37,451	41,414	39,080	43,819
		(a)	(b)	(c)	(cd)	(de)	(e)
	CI	−1,447	−5,419	−3,797	−3,790	−782	−10,972
		+3,161	+582	+7,462	+3,810	+352	+6,387
	Mean (MPa)	**27,849**	**32,573**	**38,368**	**41,418**	**38,972**	**42,672**
		(2)	**(5)**	**(3)**	**(0)**	**(0)**	**(4)**
	G_{23}' (MPa)	12,788	14,928	15,074	15,379	15,695	17,140
		(a)	(b)	(b)	(b)	(b)	(c)
	$G_{12} = G_{13}$ (MPa)	126,575	14,738	15,834	16,716	15,572	16,998
		(a)	(b)	(bc)	(bc)	(c)	(c)
	CI	−135	−1,834	−3,117	−3,473	−168	−1,590
		+396	+2,212	+1,598	+799	+412	+1,874
	Mean (MPa)	**12,722**	**14,833**	**15,454**	**16,048**	**15,634**	**17,069**
		(1)	**(1)**	**(3)**	**(6)**	**(1)**	**(1)**
	$\nu_{21} = \nu_{31}$	0.10 (Aa)	0.11 (Ba)	0.29 (Cb)	0.26 (Db)	0.25 (Fb)	0.28 (Gb)
		(31)	(5)	(8)	(8)	(6)	(5)
	$\nu_{12} = \nu_{13}$	0.11 (Aa)	0.10 (Ba)	0.31 (Cb)	0.26 (Db)	0.25 (Fb)	0.26 (Gb)
		(30)	(11)	(20)	(2)	(5)	(10)
	$\nu_{32} = \nu_{23}$	0.09 (Aa)	0.11 (Ba)	0.24 (Cb)	0.32 (Ebc)	0.25 (Fbc)	0.26 (Gc)
		(39)	(81)	(13)	(9)	(13)	(9)
	Mean	**0.10**	**0.11**	**0.28**	**0.28**	**0.25**	**0.26**
		(11)	**(4)**	**(12)**	**(13)**	**(2)**	**(4)**

Table 4. (*Continued*.)

Anisotropy condition	Elastic parameters	18 MPa (G0)	21 MPa (G1)	28 MPa (G0)	30 MPa (G1)	35 MPa (G0)	34 MPa (G1)
Isotropy	E (MPa)	27,762 (a) (4)	32,782 (b) (1)	39,394 (c) (6)	41,565 (c) (6)	39,091 (c) (1)	42,365 (c) (7)
	G (MPa)	12,702 (a) (1)	14,800 (b) (6)	15,574 (bc)	16,263 (bc) (6)	15,613 (cd) (1)	17,045 (d) (5)
	ν	0.09 (a) (43)	0.11 (a) (30)	0.26 (b) (2)	0.28 (b) (1)	0.25 (b) (1)	0.24 (b) (22)

Note: Values in parentheses indicate coefficients of variation (%). Different uppercase letters indicate significantly different values between the same parameters in lines, and lowercase letters indicate significantly different values between the parameters in columns. In this case, CI = confidence interval of the difference of the means; E_1, E_2, and E_3 = elasticity moduli of the concrete in Directions 1, 2, and 3, respectively [Fig. 1(c)]; G_{23}, G_{13}, and G_{12} = shear moduli on Planes 2-3, 1-3, and 1-2, respectively [Fig. 1(c)]; ν_{21}, ν_{31}, ν_{12}, ν_{32}, ν_{13}, and ν_{23} = Poisson's ratios on Planes 2-1, 3-1, 1-2, 3-2, 1-3, and 2-3, respectively [Fig. 1(c)]; E_1' and $E_2 = E_3$ = elasticity moduli of the concrete in Directions 1 and $2 = 3$, respectively [Fig. 1(c)]; G_{23}' and $G_{12} = G_{13}$ = shear moduli on Planes 2-3 and 1-2 = 1-3, respectively [Fig. 1(c)]; $\nu_{21} = \nu_{31}$, $\nu_{12} = \nu_{13}$, and $\nu_{32} = \nu_{23}$ = Poisson's ratios on Planes 2-1 = 3-1, 1-2 = 1-3, and 3-2 = 2-3, respectively [Fig. 1(c)]; E = elasticity moduli of the concrete in Directions 1 = 2 = 3 [Fig. 1(c)]; G = shear moduli on Planes 2-3 = 1-3 = 1-2 [Fig. 1(c)]; and ν = Poisson's ratios on Planes 2-1 = 3-1 = 1-2 = 1-3 = 3-2 = 2-3 [Fig. 1(c)]. The bold values are the means and coefficient of variation (in brackets) of the general values presented and their significance are done by the coefficient of variation.

18 and 21 MPa. For the other strengths, the mean Poisson's ratio was 0.27 (Table 4).

The Brazilian Standard for Concrete Structures Design [ABNT NBR 6118 (ABNT 2014)] proposes a fixed value of 0.2 for the Poisson's ratio of concrete. The data from this study showed that the value for this parameter varies with the strength of the concrete, which can have important implications if it is necessary to use this elastic coefficient in computational simulations for structural analyses, in which precise values are crucial for obtaining accurate results. Wang et al. (2015) determined the elastic properties of concrete with a compressive strength of 22.6 MPa using dynamic tests, and they obtained mean values for the longitudinal and transverse moduli of elasticity of 29,000 and 11,700 MPa, respectively, and a Poisson's ratio coefficient of 0.18.

The coefficients of variation of the mean elasticity moduli, for each mixture had values between 1% and 4%, whereas the coefficients of variation of the mean shear moduli were between 1% and 5% (Table 4). The coefficients of variation for the mean Poisson's ratio of each mixture had higher values, from 4% to 20% (Table 4). Wang et al. (2015) obtained values of 1.3% and 1.2% for the coefficients of variation of the mean elasticity moduli and the mean shear moduli, respectively, from the dynamic characterization of concrete. The same authors, as well as the authors of this study, also obtained higher values for the coefficient of variation of the mean Poisson's ratio (5.1%) (Wang et al. 2015).

Within the limited range investigated here, the low values for the coefficients of variation of the means of the elastic parameters [moduli of elasticity (E_1, E_2, and E_3) and shear moduli (G_{23}, G_{13}, and G_{12})] obtained in this study, which considered three axes of symmetry (orthotropic material), provide evidence for the isotropy of the concrete (Table 4).

The statistical analysis of the means of the elasticity moduli and shear moduli did not indicate statistically significant differences at the 95% confidence level for the three evaluated directions (1, 2, and 3) (Table 4). Only the Poisson's ratios ν_{32} and ν_{23} of the concrete, with its compressive strength of 25 MPa and production from Gravel 1, were significantly different from the Poisson's ratios on the other planes (ν_{21}, ν_{31}, ν_{12}, and ν_{13}; Table 4).

The characterization performed by simplifying the anisotropy of the concrete and when considering it as a transverse isotropic material, where Axis 1 (compaction direction) had different properties from Axes 2 and 3 (which had similar properties), resulted in mean moduli of elasticity varying from 27,400 to 43,800 MPa (Table 4), and the variation was a function of the compressive strength of the concrete and the type of gravel used in the mixture. The shear moduli under these conditions varied from 12,700 to

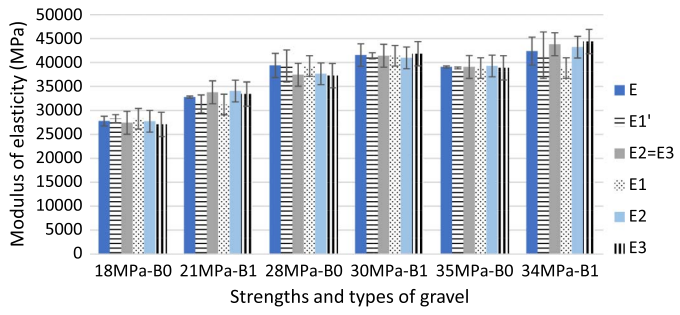

Fig. 4. Mean moduli of elasticity and standard deviations obtained when considering the concrete to have different anisotropy conditions where E is the elasticity modulus obtained from the characterization when considering the concrete as an isotropic material; E_1' and $E_2 = E_3$ are the elasticity moduli obtained from the characterization when considering the concrete as a material with transverse isotropy; and E_1, E_2, and E_3 are the elasticity moduli obtained from the characterization when assuming the concrete is an orthotropic material.

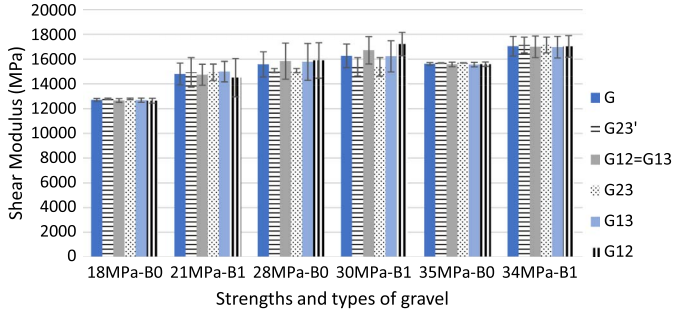

Fig. 5. Mean shear moduli and standard deviations obtained when considering the concrete to have different anisotropy conditions where G is the shear modulus obtained from the characterization when considering the concrete as an isotropic material; G_{23}' and $G_{12} = G_{13}$ are the shear moduli obtained from the characterization when considering the concrete as a material with transverse isotropy; and G_{23}, G_{13}, and G_{12} are the shear moduli obtained from the characterization when assuming the concrete as an orthotropic material.

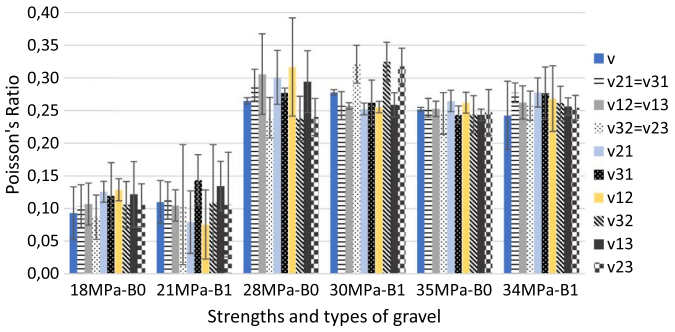

Fig. 6. Mean Poisson's ratios and standard deviations obtained when considering the concrete to have different anisotropy conditions where ν is the Poisson's ratio obtained by the characterization when assuming the concrete is an isotropic material; $\nu_{21} = \nu_{31}$, $\nu_{12} = \nu_{13}$ and $\nu_{32} = \nu_{23}$ are Poisson's ratios obtained from the characterization considering the concrete as a material with transverse isotropy; and ν_{21}, ν_{31}, ν_{12}, ν_{32}, ν_{13}, and ν_{23} are Poisson's ratios obtained from the characterization assuming the concrete is an orthotropic material.

17,100 MPa (Table 4). The Poisson's ratios ranged from 0.09 to 0.32, and the values were below 0.11 (mean of 0.10) only for the concretes with compressive strengths of 18 and 21 MPa. For the other study strengths, the mean Poisson's ratio was 0.27 (Table 4).

Similar to the characterization that considered the concrete as an orthotropic material, the means of the elastic parameters [moduli of elasticity (E), shear moduli (G), and Poisson's ratios (ν)] when considering the concrete to have transverse isotropy also had low coefficients of variation, which also indicates the isotropy of the concrete (Table 4).

The confidence intervals for the difference between the means of the elasticity and shear moduli were zero, regardless of the strength or type of gravel used in the concrete, which indicates that there was no difference between the parameters in the two evaluated directions (1 and 2 = 3) at a confidence level of 95%. The results of the statistical analysis on the difference in the Poisson's ratio means show that for all of the compressive strengths and aggregate sizes (G0 and G1) used in the mixture, there were no significant differences between the parameters in the different planes evaluated in this paper (Table 4).

Finally, the analysis of the elastic behavior of the concrete was performed by considering it to be an isotropic material. For this analysis, the moduli of elasticity (E) varied from 27,800 (strength of 18 MPa) to 42,400 MPa (strength of 34 MPa), and the shear moduli (G) ranged from 12,700 (strength of 18 MPa) to 17,000 MPa (strength of 34 MPa) (Table 4). Similar to when the concrete was analyzed as an orthotropic material or as having transverse isotropy, the Poisson's ratios were low (mean of 0.10) for strengths of 18 and 21 MPa and ranged from 0.24 (strength of 34 MPa) to 0.28 (strength of 30 MPa) for the highest strengths (greater than 28 MPa) (Table 4).

A joint evaluation of the parameters obtained from the different anisotropy conditions (orthotropy, transverse isotropy, and isotropy) shows that the variation in the parameters within each strength class and type of gravel (G0 or G1) was random with no trends that depended on the type of anisotropy assumed for the material (Figs. 4–6). The coefficients for variation for the elasticity moduli were obtained by considering the different types of anisotropy ranging from 0.4% (strength of 35 MPa) to 4.7% (strength of 34 MPa), whereas those of the shear moduli varied from 0.4% (strength of 34 and 35 MPa) to 4.5% (strength of 30 MPa) (Figs. 4 and 5). The Poisson's ratios had higher coefficients of variation (COV) according to the type of anisotropy considered during the characterization of the concrete (the COVs ranged from 3.1% to 19.2%), and the highest values were obtained for the concretes with lower strengths (18 and 21 MPa) (Fig. 6).

The mean standard deviation of the elasticity moduli was lower when the characterization was performed by considering the concrete as an orthotropic material (1,515 MPa). The lowest mean standard deviation of the shear moduli was obtained when the material characterization was performed by considering the concrete to be a transverse isotropic material (621 MPa). The lowest mean standard

Table 5. Relationship between the elasticity moduli (longitudinal and transverse) and coefficients of variation considering analyses of concrete with different types of anisotropy

Anisotropy condition	Ratio between moduli	15 MPa (G0)	15 MPa (G1)	25 MPa (G0)	25 MPa (G1)	35 MPa (G0)	35 MPa (G1)
Orthotropy	G_{23}/E_1	0.5	0.5	0.4	0.4	0.4	0.4
	G_{13}/E_1	0.4	0.5	0.4	0.4	0.4	0.4
	G_{12}/E_1	0.4	0.5	0.4	0.4	0.4	0.4
	G_{23}/E_2	0.5	0.4	0.4	0.4	0.4	0.4
	G_{13}/E_2	0.5	0.4	0.4	0.4	0.4	0.4
	G_{12}/E_2	0.5	0.4	0.4	0.4	0.4	0.4
	G_{23}/E_3	0.5	0.4	0.4	0.4	0.4	0.4
	G_{13}/E_3	0.5	0.4	0.4	0.4	0.4	0.4
	G_{12}/E_3	0.5	0.4	0.4	0.4	0.4	0.4
	Mean	**0.5**	**0.4**	**0.4**	**0.4**	**0.4**	**0.4**
	COV (%)	**2**	**6**	**3**	**5**	**1**	**6**
Transverse isotropy	G'_{23}/E'_1	0.5	0.5	0.4	0.4	0.4	0.4
	$G_{12} = G_{13}/E'_1$	0.4	0.5	0.4	0.4	0.4	0.4
	$G'_{23}/E_2 = E_3$	0.5	0.4	0.4	0.4	0.4	0.4
	$G_{12} = G_{13}/E_2 = E_3$	0.5	0.4	0.4	0.4	0.4	0.4
	Mean	**0.5**	**0.5**	**0.4**	**0.4**	**0.4**	**0.4**
	COV (%)	**2**	**4**	**4**	**5**	**1**	**3**
Isotropy	G/E	0.5	0.5	0.4	0.4	0.4	0.4

Note: E_1, E_2, and E_3 = elasticity moduli of the concrete in Directions 1, 2, and 3, respectively [Fig. 1(c)]; G_{23}, G_{13}, and G_{12} = shear moduli on Planes 2-3, 1-3, and 1-2, respectively [Fig. 1(c)]; E'_1 and $E_2 = E_3$ = moduli of elasticity of the concrete in Directions 1 and 2 = 3, respectively [Fig. 1(c)]; G'_{23} and $G_{12} = G_{13}$ = shear moduli on Planes 2-3 and 1-2 = 1-3, respectively [Fig. 1(c)]; E = elasticity moduli of the concrete in Directions 1 = 2 = 3 [Fig. 1(c)]; G = shear moduli on Planes 2-3 = 1-3 = 1-2 [Fig. 1c]; and ν = Poisson's ratios on Planes 2-1 = 3-1 = 1-2 = 1-3 = 3-2 = 2-3 [Fig. 1c]. The values in bold represent the means values and the COV of the means (in brackets) that indicate the mean significance.

deviation of Poisson's ratio was obtained by assuming the concrete to be a transverse isotropic or isotropic material. Thus, no theoretical assumption about the elastic behavior of the concrete (orthotropy, transverse isotropy, or isotropy) produced more precise values for the elastic parameters when the concrete was characterized by ultrasound.

For isotropic materials, the constitutive relation between the elasticity moduli is used [transverse (G), longitudinal (E), and Poisson's ratios (ν) are given by $G = E/2\,(1 + \nu)$]. The G/E ratios had values close to 0.4 for all of the theoretical elastic behaviors, and for most cases, the ratio was independent of the concrete strength or the dimensions of the coarse aggregate used in the mixture (Table 5). This result ($G/E = 0.4$) was obtained using the expected constitutive relation for isotropic materials when Poisson's ratio is 0.20. Wang et al. (2015) also calculated a value of 0.4 for the ratio between the elasticity modulus and the shear modulus of concrete.

The statistical differentiation between the elastic properties of concrete for the different compressive strengths and types of gravel used in its production was the same regardless of the theoretical elastic behavior assumed for the concrete (Table 4). In general, the statistical analysis divided the elasticity moduli into three groups, with one for the compressive strength of 18 MPa, another for the compressive strength of 21 MPa and a third for the other compressive strengths (28, 30, 35, and 34 MPa). Thus, regardless of the type of elastic behavior assumed in this study, the longitudinal modulus of elasticity does not have a statistically significant growth at compressive strengths above approximately 28 MPa (Table 4). The comparison of the means of the shear moduli differentiated between two primary groups, with one for the strength of 18 MPa and another for the other strengths, regardless of the type of elastic behavior assumed (Table 4). A comparison of the Poisson's ratio means also identified two primary groups, with one for compressive strengths of 18 and 21 MPa and another for the other compressive strengths, regardless of the type of assumed elastic behavior (Table 4).

Conclusion

The isotropic behavior of concrete was analyzed using ultrasound wave propagation, and the results showed that there were no statistically significant differences between the three symmetry axes, validating the classification as isotropic material. The constitutive relation between the shear and longitudinal moduli, which involves Poisson's ratio, presented a constant value independent of the type of anisotropic behavior adopted for concrete, which is expected for isotropic materials. The elastic properties of concrete differed equally as a function of the compressive strength, independent of the type of anisotropic behavior adopted for concrete.

Acknowledgments

The authors would like to thank the Support Fund for Teaching, Research and Extension (FAEPEX) for the scholarship, the São Paulo Research Foundation (FAPESP), São Paulo, Brazil (Proc. 2016/00658-4) for the research funding and the Coordination of Improvement of Higher-Level Personnel (CAPES, Brazil) for financing part of this study.

References

ABNT (Associação Brasileira de Normas Técnicas). 2009a. *Agregado miúdo—Determinação da massa específica e massa específica aparente [Small aggregate—Specific density and apparent density determination]*. ABNT NBR NM 52. Rio de Janeiro, Brazil: ABNT.

ABNT (Associação Brasileira de Normas Técnicas). 2009b. *Agregados para concreto—Especificação [Aggregates for concrete—Specification]*. ABNT NBR 7211. Rio de Janeiro, Brazil: ABNT.

ABNT (Associação Brasileira de Normas Técnicas). 2014. *Projeto de estruturas de concreto—Procedimento [Design of concrete structures—Procedure]*. ABNT NBR 6118. Rio de Janeiro, Brazil: ABNT.

ABNT (Associação Brasileira de Normas Técnicas). 2015. *Concreto—Procedimento para moldagem e cura de corpos de prova [Concrete—Procedure for molding and curing concrete test specimens]*. ABNT NBR 5738. Rio de Janeiro, Brazil: ABNT.

ABNT (Associação Brasileira de Normas Técnicas). 2018a. *Cimento portland—Requisitos [Portland cement—Requirements]*. ABNT NBR 16697. Rio de Janeiro, Brazil: ABNT.

ABNT (Associação Brasileira de Normas Técnicas). 2018b. *Concreto—Ensaios de compressão de corpos-de-prova cilíndricos [Concrete—Compression tests of cylindrical specimens]*. ABNT NBR 5739. Rio de Janeiro, Brazil: ABNT.

ABNT (Associação Brasileira de Normas Técnicas). 2019. *Concreto endurecido—Determinação da velocidade de propagação da onda ultrassônica [Hardened concrete—Determination of ultrasonic wave transmission velocity]*. ABNT NBR 8802. Rio de Janeiro, Brazil: ABNT.

Agrawal, M., A. Prasad, J. R. Bellare, and A. A. Seshia. 2016. "Characterization of mechanical properties of materials using ultrasound broadband spectroscopy." *Ultrasonics* 64 (Jan): 186–195. https://doi.org/10.1016/j.ultras.2015.09.001.

Bauer, L. A. F. 2008. *Materiais de Construção [Construction materials]*. Rio de Janeiro, Brazil: Livros Técnicos e Científicos.

Bernard, S., Q. Grimal, and P. Laugier. 2014. "Resonant ultrasound spectroscopy for viscoelastic characterization of anisotropic attenuative solid materials." *J. Acoust. Soc. Am.* 135 (5): 2601–2613.https://doi.org/10.1121/1.4869084.

Bertoldo, C., R. Gonçalves, E. S. Merlo, O. Santaclara, M. Ruy, and M. E. M. Moreira. 2013. "Elastic constants of *Pinus pinaster* wood determined by wave propagation." In *Proc., 18th Int. Nondestructive Testing and Evaluation of Wood Symp.* Madison, WI: USDA Forest Service and Forest Products Laboratory.

Cicekli, U., G. Z. Voyiadjis, and A. K. R. Al-Rub. 2007. "A plasticity and anisotropic damage model for plain concrete." *Int. J. Plast.* 23 (10–11): 1874–1900.https://doi.org/10.1016/j.ijplas.2007.03.006.

Figueiredo, E. P. 2005. Vol. 2 of *Inspeção e diagnóstico de estruturas de concreto com problemas de resistência, fissuras e deformações. Concreto: Ensino, pesquisa e realizações [Inspection and diagnosis of concrete structures with resistance problems, cracks and deformations. Concrete: Teaching, research and achievements]*, 985–1015. São Paulo, Brazil: IBRACON.

François, M. 1995. "Identification des symétries matérielles de matériaux anisotropes." Doctoral thesis. Sciences de l'ingénieur [Physics], Univ. of Paris.

François, M. L. M., G. Geymonat, and Y. Berthaud. 1998. "Determination of the symmetries of an experimentally determined stiffness tensor; application to acoustic measurements." Accessed May 16, 2018. http://search.ebscohost.com/login.aspx?direct=true&db=edsarx&AN=edsarx.0911.5216&lang=pt-br&site=eds-live&scope=site.

Gonçalves, R., A. Trinca, and D. Cerri. 2011. "Comparison of elastic constants of wood determined by ultrasonic wave propagation and static compression testing." *Wood Fiber Sci.* 43 (1): 64–75.

Gonçalves, R., A. Trinca, and B. Pellis. 2014. "Elastic constants of wood determined by ultrasound using three geometries of specimens." *Wood Sci. Technol.* 48 (2): 269–287.

Heyliger, P., A. Jilani, H. Ledbetter, R. G. Leisure, and C. L. Wang. 1993. "Elastic constants of isotropic cylinders using resonant ultrasound." *J. Acoust. Soc. Am.* 94 (3): 1482–1487. https://doi.org/10.1121/1.408151.

Hughes, B. P., and J. E. Ash. 1970. "Anisotropy and failure criteria for concrete." *Matériaux Constr.* 3 (6): 371–374. https://doi.org/10.1007/BF02478760.

Isaak, D. G., and I. Ohno. 2003. "Elastic constants of chrome-diopside: Application of resonant ultrasound spectroscopy to monoclinic

single-crystals." *Phys. Chem. Miner.* 30 (7): 430–439. https://doi.org/10.1007/s00269-003-0334-2.

Isaia, G. C. 2017. *Materiais de construção civil e princípios de ciência e engenharia de materiais.* São Paulo, Brazil: Brazilian Concrete Institute.

Liu, X., and V. Shapiro. 2017. "Sample-based synthesis of two-scale structures with anisotropy." *Comput.-Aided Des.* 90 (Sep): 199–209. https://doi.org/10.1016/j.cad.2017.05.013.

Martinović Sanja, P., M. Vlahović Milica, B. Majstorović Jelena, and T. D. Volkov-Husović. 2016. "Anisotropy analysis of low cement concrete by ultrasonic measurements and image analysis." *Sci. Sintering* 48 (1): 57–70. https://doi.org/10.2298/SOS1601057M.

Maynard, J. D. 1992. "Resonant ultrasound spectroscopy for viscoelastic characterization of anisotropic attenuative solid materials." *Acoust. Soc. Am.* 135 (5): 2601–2613. https://doi.org/10.1121/1.4869084.

Maynard, J. D., and G. Liu. 2012. "Measuring elastic constants of arbitrarily shaped samples using resonant ultrasound spectroscopy." *J. Acoust. Soc. Am.* 131 (3): 2068–2078. https://doi.org/10.1121/1.3677259.

Migliori, A., and J. P. Maynard. 2005. "Implementation of a modern resonant ultrasound spectroscopy system for the measurement of the elastic moduli of small solid specimens." *Rev. Sci. Instrum.* 76 (12): 121301. https://doi.org/10.1063/1.2140494.

Migliori, A., J. L. Sarrao, W. M. Visscher, T. M. Bell, M. Lei, Z. Fisk, and R. G. Leisure. 1993. "Resonant ultrasound spectroscopic techniques for measurement of the elastic moduli of solids." *Phys. B: Phys. Condens. Matter* 183 (1): 1–24. https://doi.org/10.1016/0921-4526(93)90048-B.

Papa, E., and A. Taliercio. 1996. "Anisotropic damage model for the multiaxial static and fatigue behaviour of plain concrete." *Eng. Fract. Mech.* 55 (2): 163–179. https://doi.org/10.1016/0013-7944(96)00004-5.

Pereira, E., and M. H. F. Medeiros. 2012. "Pull off test to evaluate the compressive strength of concrete: An alternative to Brazilian standard techniques." *Rev. IBRACON Estruturas e Materiais* 5 (6): 757–780. https://doi.org/10.1590/S1983-41952012000600003.

Rashid, Y. R. 1968. "Ultimate strength analysis of prestressed concrete pressure vessels." *Nucl. Eng. Des.* 7 (4): 334–344. https://doi.org/10.1016/0029-5493(68)90066-6.

Seiner, H., L. S. P. Bodnárová, A. Kruisová, M. Landa, A. Pablos, and M. Belmonte. 2012. "Sensitivity of the resonant ultrasound spectroscopy to weak gradients of elastic properties." *J. Acoust. Soc. Am.* 131 (5): 3775–3785. https://doi.org/10.1121/1.3695393.

Torrenti, J. M., G. Pijaudier-Cabot, and J. M. Reynouard. 2013. *Mechanical behavior of concrete*. Hoboken, NJ: Wiley. https://doi.org/10.1002/9781118557587.

Trinca, A. J. 2011. "Metodologia para determinação das constantes elásticas da madeira por ultrassom." Doctoral thesis, School of Agricultural Engineering, Univ. of Campinas.

Ulrich, T., K. R. Mccall, and R. A. Guyer. 2002. "Determination of elastic moduli of rock samples using resonant ultrasound spectroscopy." *J. Acoustic Soc. Am.* 111 (4): 1667–1674. https://doi.org/10.1121/1.1463447.

Vázquez, C., R. Goncalves, C. Bertoldo, V. Bano, A. Vega, J. Crespo, and M. Guaita. 2015. "Determination of the mechanical properties of *Castanea sativa Mill*. using ultrasonic wave propagation and comparison with static compression and bending methods." *Wood Sci. Technol.* 49 (3): 607–622. https://doi.org/10.1007/s00226-015-0719-7.

Wang, Z., Z. Gao, Y. Wang, Y. Cao, G. Wang, B. Liu, and Z. Wang. 2015. "A new dynamic testing method for elastic, shear modulus and Poisson's ratio of concrete." *Constr. Build. Mater.* 100 (Dec): 129–135. https://doi.org/10.1016/j.conbuildmat.2015.09.060.